IEEE Access
Multidisciplinary | Rapid Review | Open Access Journal

Received April 30, 2020, accepted May 27, 2020, date of publication June 1, 2020, date of current version June 22, 2020.

Digital Object Identifier 10.1109/ACCESS.2020.2999078

An Automated Method for Detection and Enumeration of Olive Trees Through Remote Sensing

MUHAMMAD WALEED[1], TAI-WON UM[2], AFTAB KHAN[3], AND ZUBAIR AHMAD[4]

[1]Department of Information and Communication Engineering, Chosun University, Gwangju 61452, South Korea
[2]Department of Cyber Security, Duksung Women's University, Seoul 01369, South Korea
[3]Department of Computer Systems Engineering, University of Engineering and Technology (UET) at Peshawar, Peshawar 25120, Pakistan
[4]Department of Mechatronics Engineering, University of Engineering and Technology (UET) at Peshawar, Peshawar 25120, Pakistan

Corresponding author: Tai-Won Um (twum@duksung.ac.kr)

This work was supported by the National Research Foundation (NRF) of Korea Grant funded by the Korea Government(MSIT) under Grant 2018R1A2B2003774.

ABSTRACT Country olive forests are one of the major contributors with economic aspects. Spain is the leading country in the world which produced around 45% of olive oil compared to the total production in the world. The value of 2.4 million hectares of land is dedicated to olive cultivation in the country, which made it a huge olive oil producer in the world. Olive crop widely spread over large extensive areas; manual counting of trees is humanly infeasible. To address this problem, we propose an automatic scheme for the detection and enumeration of olive trees. The proposed technique comprises of multi-step image processing techniques applied over a single band of imagery. The single red band once extracted from the color spectrum of acquired images, is then sharpened and edges are detected. The closed edges formed by the tree boundaries are transformed into white blobs using morphological reconstruction. Resulting circular blobs are then filtered out based on their shape and size. Blobs with circular geometry and in-range radius are considered as olive trees, which are then mapped with the existing ground information. Results have been generated over the diverse images capturing the ground truth information with an estimation error of 1.27%.

INDEX TERMS Red band extraction, image enhancement, Sobel edge detection, remote sensing.

I. INTRODUCTION

Olive fruit is having a fascinating 6000 year-long history documented by tradition and archaeological discoveries, tracing back its origin to Middle East [1]. Favorable climate conditions offered by the Mediterranean environment, olive cultivation has extended to numerous countries particularly towards Spain, France, Italy, Egypt, Portugal and some territories of Greece and Turkey. It plays an important role and contributes a lot to the country's economy like Spain, Italy, and Greece. Spain is the leading country in the world which produced 45% of olive oil and it is a major source of its economy. With the value of 2.4 million hectares of land is dedicated to the olive cultivation in the country, which made it a huge olive oil producer in the world [2]. An economically significant crop spread over wide areas, it is thus important to keep a record of their numbers maintaining their repository [3]. Manual tree count for crop estimation over such large areas is time-consuming and humanly infeasible.

In recent years, the advancements in image processing techniques and easy accessibility to Very High Resolution (VHR) satellite imagery opened its doors for remote detection of ground data. Various techniques can be used in order to detect olive trees like image segmentation, template matching, blob detection, and machine learning particularly supervised learning. In a narrow picture of image processing the segmentation techniques such as thresholding, morphological operations, region growing, clustering and edge detection are used individually or in a hybrid manner.

Thresholding is one of the simplest image segmentation technique, categorizing pixel values over a threshold level. An object thresholding-based method has been devised to detect olive trees in the province of Italy. Each of the segments formed as a result of thresholding is then identified to be

The associate editor coordinating the review of this manuscript and approving it for publication was Shiqi Wang.

a single tree or a merged tree, based on the size. Thresholding is a time-efficient technique however trading-off with accuracy. Like thresholding, region growing is also an image segmentation technique that forms the boundary extended over pixels with similar values. A combination of techniques like thresholding, region growing, and morphological operations of opening and closing is used to detect olive trees [4]. The image segmentation techniques are simple and less time consuming however, raise a concern of false detection. The template matching is a widely used technique, which is based on the detection of objects that successfully match the predefined template.

Clustering is also done to extract the region of interest by grouping pixels together based on their likelihood in intensity levels. K-means clustering is performed to detect the olive trees in a Very High Resolution (VHR) imagery [5]. However, it may fall short in separating components with similar intensity levels resulting within the same cluster. A probabilistic approach is proposed detecting olive trees planted in a distinct formation [6]. The technique is simple and robust yet shows limitation when it comes to the irregular and complex formation.

In the aerial imagery, trees exhibit a blob-like appearance which is exploited by the application of local spatial maxima to detect the olive trees [7]. However, many non-olive tree small-sized objects are counted as false positives. Blob detection combined with red band and Normalized Difference Vegetation Index (NDVI) based thresholding is proposed in [8]. The hybrid technique leads to good results but maximized the computational complexity which cannot be categorized as an efficient system. Classification is the categorization of data based on their similarities in feature space. For the classification of the olive trees, Gaussian Process Classifier (GPC) were utilized to properly classify the trees [9]. An object-based classification technique is proposed to detect olive trees using VHR imagery and radar data in [10], which shows good outcomes but with some limitations as the classifier needs to be trained with the large dataset.

This paper discusses the automatic method for olive tree detection through multiple steps of image enhancement and edge detection. High contrast between the foreground trees and background is observed in the red band of color spectrum. In accordance to which, our method utilizes only the single red band-based information to detect olive trees accurately. Image over the three bands of red, green and blue is decomposed and the red band is extracted. The edges formed by the boundaries of foreground objects including olive trees are enhanced. Closed edges are morphologically reconstructed resulting in the formation of individual blobs. Morphological structure of trees from above gives a resemblance to circular geometry, thus circular blobs are considered for that matter. Extracted blobs are mapped with the ground truth data and detection results are recorded.

The performance evaluation of the proposed technique has been tested properly on the images taken from the SIGPAC viewer providing Very High Resolution (VHR) aerial view of the Spanish territory. The algorithm shows promising results in identification and enumeration of the olive trees over the acquired images. The proposed algorithm offers the following contributions.

- Designing a least complex olive tree detection system utilizing single band of image information.
- Counting of olive trees within diverse set of images both in terms of number of samples and ground classes.

The rest of the paper is organized as follows: Section 2 discusses the previous work done in the detection and enumeration of olive trees. Section 3 explains the methodology and stepwise execution of the algorithm. Section 4 covers the results and experimentation over the dataset and the accuracy assessment of the algorithm. In the end, section 5 concludes the paper, followed by future work.

II. RELATED WORK

The automatic identification of trees using remote sensing was originally proposed for forestry applications [11]. However, detection and enumeration of trees over crop fields have always been of high significance among the research community over the past few years. Many techniques has been proposed to address the problem of the identification and enumeration of the olive trees effectively. The suggested techniques for the stated problem are discussed in groups based on the governing methods of image processing.

A. IMAGE SEGMENTATION

Yahn H. Chemin and Pieter S.A. Beck proposed an automatic method of detecting and counting olive trees a. The technique was tested over the territory of Apuglia, Italy. The aerial images were collected using large format photogrammetric cameras with Near Infra-Red (NIR) sensors. They proposed the pre-processing of images to NDVI, which were then segmented based on Niblack's thresholding method and Sauvola binarization [12].

The centroids from the segments were extracted resulting in olive tree count based on the segment size. The algorithm showed promising results with an overall mean error of 13%. However, was unable to distinguish between closely planted trees. Juan Moreno-Garcia et al proposed a K-mean clustering-based algorithm to segment olive trees from the VHR satellite imagery of Spain [5]. The tests were performed on part of the aerial imagery with a value of k set to 2 and 3.

The proposed method was fast over a smaller number of clusters and was able to distinguish between the ground data. The methodology resulted in omission rate of 0 and a commission rate of 1 in 6. Despite the promising results, the tested images were not adequate enough in terms of number and diversity. Also, the algorithm was unable to distinguish between the joint tree crowns causing miscalculation of results. OLICOUNT tool was developed to count olive trees in images having only 8-bit of information [13]. The tool relied on a combination of techniques such as thresholding, region growing, and morphological operations. The tool

was semi-automatic and required parameter tuning. As an improvement to OLICOUNT, OLICOUNT V2 integrated 16-bit of information however, tests indicated no improvement in the results.

Khan et al in [14] proposed an image segmentation technique extracting olive trees from foreground using multi-level thresholding technique. In their work, they proposed an efficient and robust model to accurately segment out and detect olive trees from the diverse environments. The technique showed promising results with an overall accuracy of 96% however, left room for further improvement due to the inclusion of non-olive elements in the tree count.

Waleed *et al.* [15] in addressed the problem of manual counting of olive trees over the large areas and proposed a technique for the detection and counting of the olive trees. The technique consists of several steps that has been utilized like pre-processing, image segmentation, feature extraction and finally classification. K-Means segmentation was utilized for the segmentation process of the region of interest. By developing various classifiers, promising results were achieved. The Random Forest classification technique shows good results with an accuracy of 97.5% for the training and testing.

Esther Salami et al in [16] presented a color segmentation based technique along with individual trees geolocation. The technique was deployed in the form of an application designed to count olive trees in aerial images. The application showed promising results by counting 330 out of 332 trees, however the combination of on-board processing capabilities combined with cloud services do not overcome the latency and computational time.

B. TEMPLATE MATCHING

J. Gonzales applied the probabilistic model for counting of olive trees by exploiting the reticular pattern of the planted trees [6]. Olive trees are planted in a reticular pattern with a spacing of 6 to 10 meters among the trees. Geometric features of shape and size of the olive tree were then extracted and the angle between the trees within the reticle was also computed.

The tests were performed over QUICKBIRD imagery. They detected the olive trees on the basis of the joint probability of a tree being in the reticular formation along with the geometric features. An average detection rate of 98% was achieved. Though, the technique showed its limitation for the irregular arrangement of trees; plantation by farmers to utilize space. Hence, it would not accurately detect olive trees that have not been planted in the same pattern.

C. BLOB DETECTION

Laplace operator or Laplacian is a differential operator given by the divergence of the gradient of a function on Euclidean space. It is mostly used for edge detection and blob detection. Local maximum points in the spatial resolution of Laplacian are extracted for the detection of the olive [7]. The proposed method was tested in IKONOS and QUICKBIRD satellite imagery. Blob detection is a very simple and robust technique, however, is prone to the commission of non-olive ground data. As a result of which many non-olive tree small sized objects were also added to the count.

Ioannis *et al.* proposed Arbor Crown Enumerator (ACE) method, a tree crown detection algorithm for multi-spectral imagery [8]. The algorithm utilized the NDVI and red band-based thresholding combined with blob detection. The algorithm addressed the shortcomings of the blob detection technique when applied solely. ACE was tested over the Keritis Watershed in the island of Crete. The QUICKBIRD multi-spectral satellite imagery covered not only the olive trees but also orange trees and vineyards. The algorithm showed promising results with an estimated error of 1.3% with an added computational complexity over four bands.

D. CLASSIFICATION

Yakoub *et al.* work proposed an automatic method for the identification of the olive trees by differentiating olive trees from other ground data objects [9]. The morphological features such as size, shape, etc. were extracted and fed into the GPC resulting in binary classification map. The classification was performed over the agricultural area in Al Jouf city, Saudi Arabia acquired from the IKONOS-2 satellite. Training and testing samples were extracted from the satellite imagery. The algorithm showed an overall detection rate of 96%, detecting 1124 trees out of 1167. The land cover classes contained soil, buildings, and other non-olive trees. Olive trees classified among the land cover classes were counted using blob analysis. The results showed a high overall accuracy however, the classifier was trained over relatively less training samples leaving the space for improvement.

Jan Peters *et al.* proposed an object-based classification of olive trees over a study region of France [10]. Synergy models were developed by combining different features from multiple sensors at different stages of object-based classification. The decision-based accuracy was obtained as 88%, relatively lower in comparison to the previous techniques.

Juan Moreno *et al.* used the fuzzy logic method to generate the fuzzy number and used it to process the olive trees imagery using k-neighbor approach [17]. The methodology was tested over VHR satellite imagery obtained from SIGPAC (Sistema de Informacion Geografica de parcelas agricolas) viewer of Ministry of Environment and Rural and Marine. Results came out to be promising, showing an omission rate of 1 in 6 and a commission rate of 0. The results were obtained with a value of k at 1 and 2. The algorithm was tested over a part of aerial imagery and diversity in the testing images was also not explained.

Work done in the literature showed the application of different techniques towards the automatic detection of olive trees. Simple and efficient techniques like image segmentation to the training and testing samples over complex classifiers, all of them showed promising results. However, it has been observed that the accuracy was achieved with the increase in the image information. Also, the utilized datasets lacked the required diversity in number and ground classes.

Our proposed algorithm focuses on achieving high accuracy with the least information available over a highly diverse environment.

III. PROPOSED METHODOLOGY

Our proposed methodology for the detection and enumeration of olive trees is shown in the Figure 1. The methodology is explained as below.

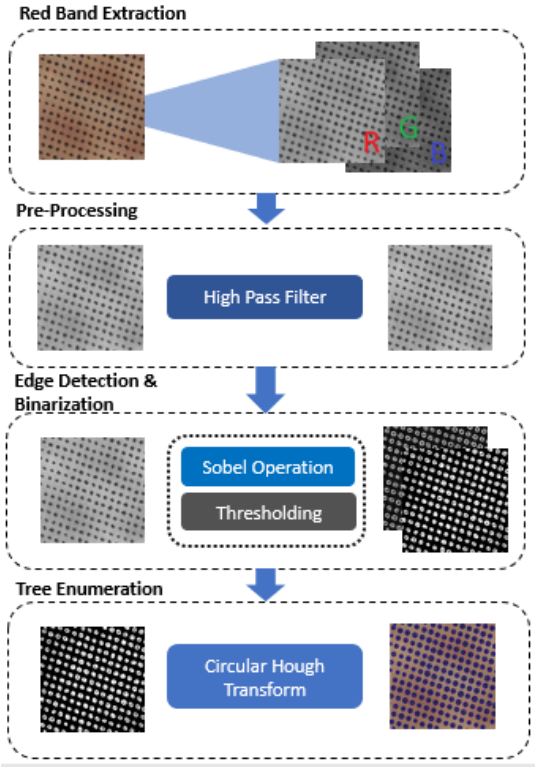

FIGURE 1. Overview of the proposed scheme.

A. IMAGE ACQUISITION

In the first step of our algorithm, color images are acquired by using the SIGPAC viewer of the Ministry of the Environment and Rural and Marine Affairs [18]. The viewer provides a VHR view of Spanish territory with a spatial resolution of 1 meter. The images are taken over the region of Castilla La-Mancha, covering the province of Toldeo. The Toledo province occupies a leading position in the Spanish industry of food and agriculture and comes second in terms of olive oil production.

B. RED BAND EXTRACTION

An image is a 2D array where each position is represented by intensity levels. RGB image or true colour image of 24-bits contains 8-bits per channel, each for red, green and blue. In other words, a true colour image is composed of three images each belonging to a distinct channel. With 8-bits per channel, each pixel can store intensity levels from 0 to 255.

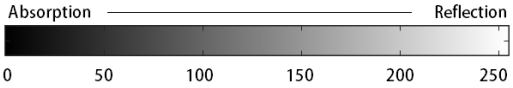

FIGURE 2. 8-bit intensity range.

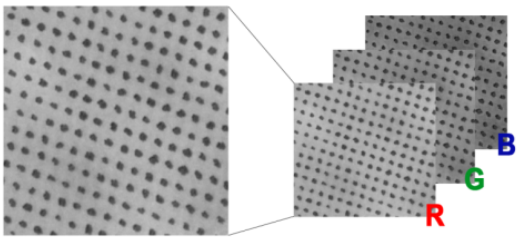

FIGURE 3. Extraction of red band from RGB image.

Over the range of 256, complete absorption occurs at 0 to a total reflection at 255 as shown in Figure 2.

When it comes to the evergreen olive trees, image pre-processing methods are applied to enhance the green vegetation in the foreground. Various metrics and methods can be used to enhance that vegetation index such as few Triangular Greenness Index [19] and Normalized Difference Vegetation Index(NDVI) [8]. According to the NDVI, the visible red band is strongly absorbed by the dense green vegetation as it is sensitive to chlorophyll. Olive trees absorb solar radiation which acts as a source of energy during photosynthesis. Since the red band is absorbed by chlorophyll therefore, red band appears to be dark [20]. The absorption of red band in case of olive trees is exploited, extracting dark pixels from the image for accurate detection and segmentation. In the colour spectrum, red band was extracted from the image by taking 8-bits of red channel from each location of the 2D image as shown in the Figure 3.

For an RGB image im having a width of j pixels and a height of i pixels, the red band $R(i, j)$ is extracted as the first band. Mathematically shown as in Equation 1 below,

$$R(i, j) = im(i, j, 1) \tag{1}$$

C. IMAGE SHARPENING

Image enhancement is to improve the information in images to achieve better results. Enhancement is required to highlight the edges formed by the dark pixels of the olive trees and other ground information. These edges are enhanced for better extraction of the olive trees in later steps. Image enhancement can be done in both spatial as well as in frequency domain. For less computational complexity and ease of manipulation, the red band image is sharpened in the frequency domain [21].

Basic steps for image enhancement in the frequency domain are as follows.

1) Acquisition of Red band image in spatial domain $f(x, y)$ having dimensions MxN.
2) Transformation of red band image $f(x, y)$ from spatial to the frequency domain, $F(u, v)$.

3) Multiplication of filter function $H(u, v)$ with the transformed red band image $F(u, v)$.
4) Inverse transformation of the sharpened red band image back to the spatial domain.

The input image in spatial domain is transformed into frequency domain using the Discrete Fourier Transform (DFT). Mathematically shown in Equation 2,

$$F(m,n)^n = \sum_{i=1}^{M}\sum_{j=1}^{N} R(i,j)e^{-i2\pi\left(\frac{mi,n\,j}{N}\right)} \tag{2}$$

1) HIGH-PASS FILTER

A high pass filter as by its name indicates attenuates the low-frequency components of the image while keeping the high-frequency components intact. We have used the Gaussian high pass filter (GHPF) in our algorithm [22]. The transfer function of GHPF is given in the Equation 3 below,

$$H(m,n) = 1/1 + \left[D_0/D(m,n)\right]^{2n} \tag{3}$$

where D_0 is the cut-off frequency, n is the order of the filter and $D(m, n)$ is the distance from the point (m, n) to the center of the filter. Mathematically shown as in Equation 4,

$$D(m,n) = \left[\left(m - \frac{M}{2}\right)^2 + \left(n - \frac{N}{2}\right)^2\right]^{1/2} \tag{4}$$

The high pass filter $H(m, n)$ was then multiplied with the red band image in frequency domain $F(m, n)$, resulting in sharpened image $G(m, n)$ as shown in the Equation 5,

$$G(m,n) = H(m,n) \times F(m,n) \tag{5}$$

The resultant filtered image was then converted back into the spatial domain by applying the Inverse Discrete Fourier Transform as shown in Equation 6,

$$Rf(i,j) = \frac{1}{MN}\sum_{m=1}^{M-1}\sum_{n=1}^{N-1} G(m,n)e^{-i2\pi\left(\frac{mi}{M}+\frac{nj}{N}\right)} \tag{6}$$

where $Rf(i, j)$ is the filtered red band image in the spatial domain.

D. EDGE DETECTION

After the red band image was sharpened and edges were enhanced, edge detection algorithms were applied to extract the edges formed by foreground information in the image. For this purpose, Sobel operators were applied on to the sharpened image $R(i, j)$.

1) SOBEL OPERATOR

Sobel operator is developed based on the idea of a 3 × 3 isotropic gradient operator [23]. It uses two 3 × 3 kernels and is convolved with the source image, the sharpened image from high pass filtration. The kernels estimate any change in both the x-axis and y-axis. Each kernel is given in Equation 7 and 8 below,

$$Kx = \begin{bmatrix} +1 & 0 & -1 \\ +2 & 0 & -2 \\ +1 & 0 & -1 \end{bmatrix} \tag{7}$$

$$Ky = \begin{bmatrix} +1 & +2 & +1 \\ 0 & 0 & 0 \\ -1 & -2 & -1 \end{bmatrix} \tag{8}$$

The approximations to the variations result information of an image, representing the edges in both axes. Edges are formed around the dark trees and the ground information due to the variation in the intensities as shown in the Equations 9 and 10 below,

$$Gx = Kx * Rf \tag{9}$$

$$Gy = Ky * Rf \tag{10}$$

where G_x and G_y are the two images corresponding to changes in the x-axis and y-axis respectively. At each point in the image, the two gradient approximations can combine to give gradient magnitude using Equation 11.

$$G = \sqrt{Gx^2 + Gy^2} \tag{11}$$

The direction of gradient at any point can be calculated using both G_x and G_y from the following Equation 12.

$$\theta = \tan^{-1}\frac{Gy}{Gx} \tag{12}$$

E. IMAGE SUBTRACTION

Image subtraction is a pixel-based operation where intensity values of one are subtracted from the intensity value of the other image as shown in Figure 4.

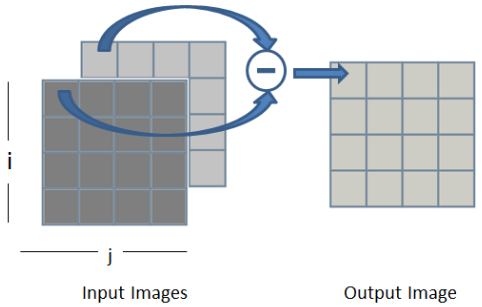

FIGURE 4. Pixel-based subtraction.

The image subtraction is primarily done to balance the uneven sections of an image adding a monotonous effect to the intensities [24]. In order to balance out the mid-gray values in the background, the filtered image $Rf(i, j)$ was subtracted pixel by pixel from the resultant image $G(i, j)$ from the Sobel operation as shown in Equation 13.

$$D(i,j) = G(i,j) - Rf(i,j) \tag{13}$$

F. IMAGE BINARIZATION

Image Binarization is the conversion of grey-scale image to binary [25]. The foreground consists of the object of interest whereas the rest becomes the background. Both classes are assigned values of 0 and 1 accordingly. Binarization step draws a line over the values of pixels by threshold, α. Pixels with luminance values greater than α are assigned 1 or 0 and vice versa. Image obtained as $D(i, j)$ in the last step is converted to binary $Db(i, j)$ as given in the Equation 14 below,

$$Db(i,j) = \begin{cases} 0, & D(i,j) < \alpha \\ 1, & D(i,j) \geq \alpha \end{cases} \tag{14}$$

G. TREE ENUMERATION

The resulting binary image Db is now used to count the number of olive trees. In this step the connected boundaries of objects are filled in by replicating the boundary pixels to the center of each object. Trees from above are visible by their circular canopy structure, thus only circular blobs were to be accounted as the olive trees. These circular blobs were detected using Circular Hough Transform (CHT).

1) CIRCULAR HOUGH TRANSFORM

Circular Hough Transform is a specialized version of Hough Transform that finds circles within an input image. The candidate circular objects are identified by a voting scheme in the Hough parameter space [26]. The circles whose points are intersected the most with the edge points are voted to be a candidate circle in the image. Once the circular white blobs are identified within the binary image Db, they are counted row by row based on their radii throughout the image.

IV. RESULTS

A. DATASET

Our dataset comprises almost 60 images collected over the territory of Spain. The images have been obtained from the SIGPAC (Sistema de Informacion Geografica de parcelas agricolas) viewer offering the VHR aerial view over the territory of Spain with a spatial resolution of 1 meter (http://sigpac.mapa.es/fega/visor/). Parameters defining the center of the area by Universal Transverse Mercator (UTM) corresponding to Huso 30 with X = 411943.23 and Y = 4406332.6 [16]. The images of size 300 × 300 were taken of the area having 24-bit of information over RGB bands. Red band of information (8 bits) was utilized in our proposed method. The dataset mainly covered the region of Castilla –La Mancha, located in the center of the Peninsula, to the south of Madrid. Images have been acquired over the region covering different ground components such as olive trees, roads, shrubs and bushes, houses and sheds, rocks and rough terrains. Among the ground information, only olive trees were labeled and marked as the desired class objects with an assistance of an expert arboriculturist. A binary mask was made highlighting only olive trees in an image sample which was then utilized for the performance evaluation of the proposed scheme. Sample images covering the mentioned cases are shown in Figure 5(a) to Figure 5(e).

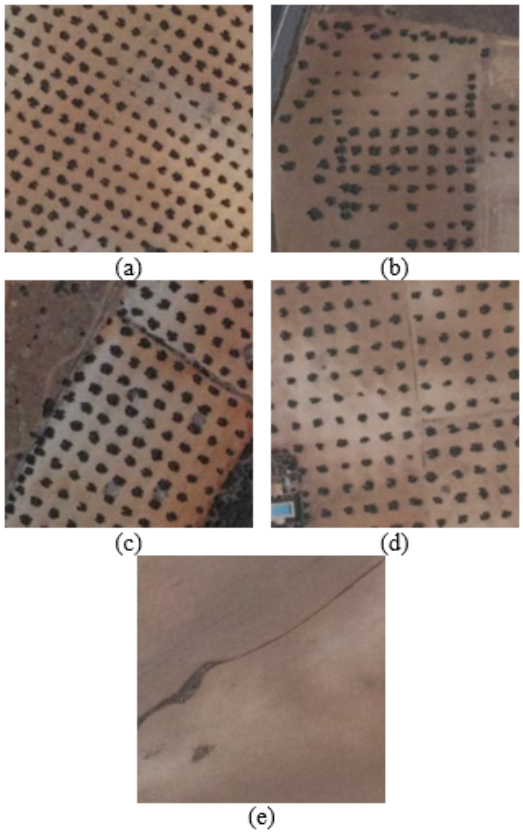

FIGURE 5. Sample images covering various case scenarios.

B. ACCURACY ASSESSMENT

In respect to the diverse dataset and posed challenges, the performance of our algorithm was tested over a set of different performance analysers.

1) ESTIMATION ERROR

It is elucidate as the inaccuracy between the estimation of information in a given sample and the actual information to be estimated. Mathematically shown in Equation 15 as,

$$e_r = N_{estimated} - N_{actual}/N_{actual} \times 100 \tag{15}$$

2) COMMISSION ERROR

It is defined as the inclusion of negative samples detected as positives. It is also known as False Positives. It occurs due to the inclusion of other than olive tree elements.

3) OMISSION ERROR

It is described as the proportion of positive test occurrences falling outside the detected data. It is also known as False Negatives. It occurs due to failure of the successful identification of olive trees excluding them from positive occurrences.

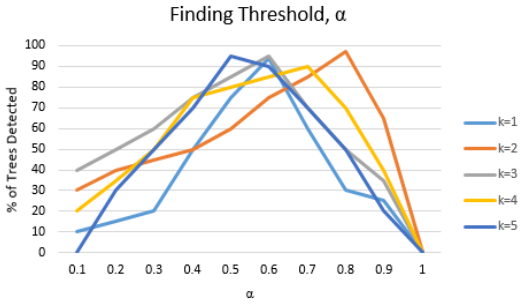

FIGURE 6. Relationship between detected trees and threshold α.

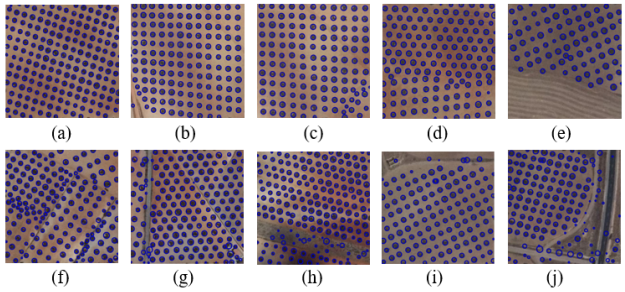

FIGURE 7. Sample images with olive trees along their estimated boundaries.

C. PARAMETER LEARNING

During the conversion of the image from grey-scale to binary, the global threshold value α for grey-scale images is calculated. If the luminance value of a given pixel is greater than that level, 1 is assigned and 0 is assigned if it is less. Binarization is a key step in our algorithm as it separates the foreground from the background thus separating the trees from the background soil of the image [27]. The optimal value of the global threshold α is selected using the trial and error method. The optimal value of α will be the one differentiating the background and foreground in such a way that a maximum number of trees are detected in the tree count. The optimal value is determined based on the maximum overlap between the segmented image and the marked ground truth data. In order to find the value of α, we have employed k-fold cross validation method where our dataset is divided into k number of groups. During each iteration, k-1 groups are utilized to determine the threshold value, holding one out for testing. Variation of α over each iteration is recorded as shown in Figure 6. Optimal values found over k number of iterations came out to be 0.6, 0.85, 0.6, 0.7 and 0.5 respectively. It has been observed that for training samples showing varying contrast, young and closely planted trees and plantation near the barren lands, threshold value came out to be comparatively low. Values greater than that caused inseparability of the intensities between foreground and background.

D. RESULTS OF OLIVE TREE DETECTION

After evaluating our proposed method over our dataset under k-fold cross validation approach results over testing samples showed an overall estimation error of 1.27%. For 100% distribution of information as 40% olive and 60% non-olive about 1.2% of non-olive data has been detected as olive and 4% of olive data has been mis-calculated as non-olive as shown in Table 1. The reason for a high omission error is due to the low threshold values calculated in the training phase leaving many positive tree samples un-extracted.

This includes a subset of images from our dataset with both best and average results showing an overall detection with an estimation error of 1.27%. Figure 7 presents a few of the sample images from each of the respective category. Images from (a) to (e) represent the tree detection map along with encircled olive trees lying within the size limits from lmin to lmax accurately detected by our system. Images from (f) to (k) represent the detected results of olive trees with the inclusion of other ground components. Figure 7(a) covered the reticular pattern of olive trees planted in the field. Result show 100% detection of olive trees with outlining each tree correctly. However, the trees lying at the border were not considered part of the final results.

Figure 7(b) again represents the reticular pattern of the olive trees with a slight variation in the angle. All the trees in the image are accurately detected and listed. Figure 7(c) presents an almost hybrid formation of the plantation pattern of olive trees. In the given image, 90% of olive trees were planted in a reticular pattern where 10% at the south-east corner were irregularly placed. The results show a 100% detection of olive trees in both patterns. In this case, again olive trees were well separated throughout the area however the trees in the south-east corner were closely planted.

Figure 7(d) presents the intersection of two separate olive tree fields varying by the angle of their reticular arrangements. In this case 99.9% of the trees were detected correctly. Figure 7(e) presents the combination of olive trees along with the freshly prepared fields ready for plantation. The trees were present in the top half section of the image and were correctly detected showing 100% detection results. All the tree sizes were in the range and were all outlined. Apart from the inclusion of other ground components, results were promising but not highly accurate reducing the detection accuracy down to 98% as shown in Figure 7(f) to Figure 7(j). Figure 7(f) covered the reticular arrangement of the olive trees with an array of shrubs and bushes in between. Results show the detection of almost 98% of the olive trees however trees in close vicinity with very small separating distance were considered as one.

Figure 7(g) present the olive trees along with shrubs and bushes, a solid road on the side and a compound at the south-east corner. The results show the detection of all the trees with the commission of a group of shrubs and bushes. The reason behind the false detection is due to the thick filled closed boundaries of the shrubs and bushes alongside the road. In Figure 7(h) reticular arrangement of olive trees are

TABLE 1. Evaluation matrix of proposed systems.

Total Trees	Detected Trees	Estimation Error	Commission Error	Omission Error
12584	12425	1.27 percent	151 (1.2 percent)	505 (4 percent)

TABLE 2. Comparative analysis of proposed scheme with benchmarks schemes.

					Performance Evaluation		
Sr. No	**Technique**	**Dataset**	**No of Images**	**Spectrum**	**CE**	**OE**	**EE**
1	Reticular Matching [6]	Quickbird	N/A	Grey-Scale	5 in 100	7 in 100	1.24%
2	Laplaican Maxima [7]	Quickbird/IKONOS	N/A	Grey-Scale	N/A	N/A	N/A
3	GPC [9]	IKONOS-2	1	RGB	N/A	N/A	3.68%
4	K-Mean Clustering [5]	SIGPAC Viewer	N/A	RGB	0 in 6	1 in 6	N/A
5	Fuzzy Logic [14]	SIGPAC Viewer	N/A	RGB	0 in 6	1 in 6	N/A
6	Red-band Thresholding + NDVI + blob detection [8]	Quickbird	10	4-bands	N/A	N/A	1.3%
7	Olive tree count in Heterogenious plantation[1]	Drone Images	4	4-bands	N/A	N/A	13%
8	Object based olive grove mapping [10]	Multi-sensor	N/A	4-bands	N/A	N/A	N/A
9	Multi-level thresholding based detection [13]	SIGPAC Viewer	95	Grey-Scale	3 in 100	3 in 100	1.2%
10	**Red Band Based Detection (Proposed)**	**SIGPAC Viewer**	**60**	**Red Band**	**1.2 in 100**	**4 in 100**	**1.27%**

found along with rough patches with shrubs and bushes. Due to rough surface in between the two olive fields, multiple edges have been detected. All the olive trees present were correctly identified however the small bushes again added false information in the tree count.

For Figure 7(i) results show the detection of almost 98% of olive trees with omitting a couple of young olive trees in the top row. Due to the presence of dense vegetation at the borders, they were considered as olives. Since our algorithm focused on the dark pixels in the red band, the dark shadow created by the compound at the north-west corner is considered too as the olive tree. For Figure 7(j) the results comply with that of the previous ones. Thick edges formed along the road side and the boundaries of the olive fields play a key role in misinterpretation of ground data. Thick vegetation alongside the edges and borders along with the dark shadows of non-olive components lead to false results.

V. DISCUSSION

A. COMPARATIVE ANALYSIS WITH BENCHMARK SCHEME

J.Gonzales used images from Quickbird satellite to detect olive trees using reticular matching. In their technique, they used the probabilistic approach exploiting the reticular pattern of the olives in which they are planted. Due to space utilization purposes, farmers may plant olive trees in an irregular formation. Karantzalos et al used the basic image processing techniques to detect the blobs created using the Laplacian maxima over the grey-scale images acquired from Quickbird and IKONOS satellites [7]. Juan Moreno Garcia worked on the VHR imagery acquired from the Sigpac viewer covering the Spanish territory [5], [14]. Their work showed the application of fuzzy logic combined with k nearest neighbor technique resulting in the detection of almost all the trees with commission and omission rates of 0 and 1 respectively in the 6 test cases.

Moreno Garcia applied the k-mean clustering testing the sample images by varying the value of k. Results showed the commission rate of 0 in all 6 cases with omission rate of 1 in 6 proofs. Yakoub et al detected olive trees using the Gaussian Process Classifier, a supervised learning technique resulting in 96% detection of the olive trees [9]. The sampled images were created having both olive and non-olive data. Supervised classification leads to better results however, their samples were not enough. Lastly, Ioannis et al used a hybrid technique combining red band thresholding with the NDVI from NIR bands and blob detection mechanism [8]. The imagery included olive trees along with fields of orange and vineyards. The technique utilized the multi-spectral imagery to correctly detect the green vegetation which resulted in detection of almost all the trees with an average estimation error of 1.3%.

A synergy based model was proposed by Jan Peters et al combining the sensor data from the multi-step classification technique [10]. The methodology was tested over the land of Southern France showing an overall accuracy of 84.3%. Chemin *et al.* proposed the technique to monitor the olive tree count as a result of loss against a deadly crop pathogen. The technique utilized a combination of thresholding and centers extraction for detection of olive trees. With a simple implementation, the algorithm showed an estimation error of 13%. Khan et al in [14] proposed an image segmentation technique extracting olive trees from foreground using multi-level thresholding technique. In their work, they proposed an efficient and robust model to accurately segment out and detect olive trees from the diverse environments. The technique showed promising results with an overall accuracy of 96% however, left room for further improvement due to the inclusion of non-olive components in the tree count.

Our images included regularly arranged as well as irregular planted olive trees. Our technique utilized a single red band of the RGB image exploiting the high contrast of vegetation in the red band for better detection. Our algorithm showed an overall estimation error of 1.27% in samples with olive trees and non-olive ground data, least among the existing techniques. Comparative analysis has been drawn among the proposed technique and existing methods as given in Table 2.

In comparison to our methodology, our dataset was made diverse covering both olive and non-olive data over 60 images within our dataset.

VI. CONCLUSION

In this paper, we have proposed a computationally efficient approach for detection and enumeration of olive trees.The proposed algorithm is composed of multiple steps tested over the territory of Toledo province in Spain. RGB images acquired through SIGPAC viewer were utilized and the red band information was extracted. In the next step, the extracted red band of information was sharpened highlighting the edges which were subtracted from the filtered image in the later step. Uneven gray tones in the background were

levelled and the resultant image was thresholded into binary. Sharp edges forming closed boundaries were morphologically reconstructed. Those boundaries formed by the closed edges were filled in replicating the boundary pixels values. The resulting blobs with circular morphology and lying in a given range of radius were considered as olive trees.The detected olive trees were mapped with the ground marked information to evaluate the performance of our algorithm. It has been concluded from our results that the trees planted in close vicinity were omitted along with the commission of non-olive trees exhibiting the morphological and geometrical features similar to that of olive trees. Due to which false positives were added to the resulting count. As a future work, we will be incorporating the morphological operators to reduce the connecting boundaries of olive trees in the close vicinity along with the incorporation of more distinctive features of olive trees.

ACKNOWLEDGMENT

The authors would like to thank the reviewers valuable time and help to improve the quality of their research work.

REFERENCES

[1] B. Khadari and A. El Bakkali, "Primary selection and secondary diversification: Two key processes in the history of olive domestication," *Int. J. Agronomy*, vol. 2018, pp. 1–9, Nov. 2018, doi: 10.1155/2018/5607903.
[2] A. Galati, G. Schifani, M. Crescimanno, D. Vrontis, and G. Migliore, "Innovation strategies geared toward the circular economy: A case study of the organic olive-oil industry," *Rivista Di Studi Sulla Sostenibilita'*, vol. 2018, no. 1, pp. 137–158, 2018.
[3] S. Peedell, S. Kay, and G. Giordino, "Computer-assisted recognition of olive trees in digital imagery," in *Proc. ESRI User Conf.*, San Diego, CA, USA, Jul. 1999, pp. 6–16.
[4] Y. H. Chemin and P. S. Beck, "A method to count olive trees in heterogenous plantations from aerial photographs," *Preprints*, vol. 2017, pp. 1–17, Oct. 2017, doi: 10.20944/preprints201710.0170.v1.
[5] J. Moreno-Garcia, L. J. Linares, L. Rodriguez-Benitez, and C. Solana-Cipres, "Olive trees detection in very high resolution images," in *Information Processing and Management of Uncertainty in Knowledge-Based Systems. Applications* (Communications in Computer and Information Science), vol. 81, E. Hüllermeier, R. Kruse, and F. Hoffmann, Eds. Berlin, Germany: Springer, 2010.
[6] J. González, C. Galindo, V. Arevalo, and G. Ambrosio, "Applying image analysis and probabilistic techniques for counting olive trees in high-resolution satellite images," in *Advanced Concepts for Intelligent Vision Systems* (Lecture Notes in Computer Science), vol. 4678, J. Blanc-Talon, W. Philips, D. Popescu, and P. Scheunders, Eds. Berlin, Germany: Springer, 2007.
[7] K. Karantzalos and D. Argialas, "Towards automatic olive tree extraction from satellite imagery," *Int. Arch. Photogramm., Remote Sens. Spatial Inf. Sci.*, vol. 35, pp. 1173–1177, Jan. 2004.
[8] I. N. Daliakopoulos, E. G. Grillakis, A. G. Koutroulis, and I. K. Tsanis, "Tree crown detection on multispectral VHR satellite imagery," *Photogramm. Eng. Remote Sens.*, vol. 75, no. 10, pp. 1201–1211, Oct. 2009, doi: 10.14358/PERS.75.10.1201.
[9] Y. Bazi, H. Al-Sharari, and F. Melgani, "An automatic method for counting olive trees in very high spatial remote sensing images," in *Proc. IEEE Int. Geosci. Remote Sens. Symp.*, Cape Town, South Africa, Jul. 2009, pp. 1–4, doi: 10.1109/IGARSS.2009.5418019.
[10] J. Peters, F. Van Coillie, T. Westra, and R. De Wulf, "Synergy of very high resolution optical and radar data for object-based olive grove mapping," *Int. J. Geographical Inf. Sci.*, vol. 25, no. 6, pp. 971–989, Jun. 2011, doi: 10.1080/13658816.2010.515946.
[11] Z. Zhen, L. Quackenbush, and L. Zhang, "Trends in automatic individual tree crown detection and delineation—Evolution of LiDAR data," *Remote Sens.*, vol. 8, no. 4, p. 333, Apr. 2016, doi: 10.3390/rs8040333.
[12] L. Zhao, S. Zheng, W. Yang, H. Wei, and X. Huang, "An image thresholding approach based on Gaussian mixture model," *Pattern Anal. Appl.*, vol. 22, no. 1, pp. 75–88, Feb. 2019, doi: 10.1007/s10044-018-00769-w.
[13] S. Bagli and V. Olicount "Technical documentation," Joint Res. Centre, Ispra, Italy, Tech. Rep. IPSC/G03/P/SKA/skaD, 2005.
[14] A. Khan, U. Khan, M. Waleed, A. Khan, T. Kamal, S. N. K. Marwat, M. Maqsood, and F. Aadil, "Remote sensing: An automated methodology for olive tree detection and counting in satellite images," *IEEE Access*, vol. 6, pp. 77816–77828, 2018, doi: 10.1109/ACCESS.2018.2884199.
[15] M. Waleed, T.-W. Um, A. Khan, and U. Khan, "Automatic detection system of olive trees using improved K-means algorithm," *Remote Sens.*, vol. 12, no. 5, p. 760, Feb. 2020.
[16] E. Salamí, A. Gallardo, G. Skorobogatov, and C. Barrado, "On-the-fly olive tree counting using a UAS and cloud services," *Remote Sens.*, vol. 11, no. 3, p. 316. 2019, doi: 10.3390/rs11030316.
[17] J. Moreno-Garcia, L. Jimenez, L. Rodriguez-Benitez, and C. J. Solana-Cipres, "Fuzzy logic applied to detect olive trees in high resolution images," in *Proc. Int. Conf. Fuzzy Syst.*, Jul. 2010, pp. 1–7, doi: 10.1109/FUZZY.2010.5584310.
[18] (2020). *Visor SigPac V 4.4*. [Online]. Available: http://sigpac.mapama.gob.es/fega/visor/
[19] B. Neupane, T. Horanont, and N. D. Hung, "Deep learning based banana plant detection and counting using high-resolution red-green-blue (RGB) images collected from unmanned aerial vehicle (UAV)," *PLoS ONE*, vol. 14, no. 10, Oct. 2019, Art. no. e0223906, doi: 10.1371/journal.pone.0223906.
[20] Z. Li, R. Hayward, J. Zhang, Y. Liu, and R. Walker, "Towards automatic tree crown detection and delineation in spectral feature space using PCNN and morphological reconstruction," in *Proc. 16th IEEE Int. Conf. Image Process. (ICIP)*, Cairo, Egypt, Nov. 2009, pp. 1705–1708, doi: 10.1109/ICIP.2009.5413642.
[21] S. Dewangan and A. Sharma, "Image smoothening and sharpening using frequency domain filtering technique," *Int. J. Emerg. Technol. Eng. Res.*, vol. 5, pp. 169–174, Apr. 2017.
[22] L. Jin, M. Jin, Z. Zhu, and E. Song, "Color image sharpening based on local color statistics," *Multidimensional Syst. Signal Process.*, vol. 29, no. 4, pp. 1819–1837, Oct. 2018, doi: 10.1007/s11045-017-0532-6.
[23] S. Israni and S. Jain, "Edge detection of license plate using Sobel operator," in *Proc. Int. Conf. Electr., Electron., Optim. Techn. (ICEEOT)*, Chennai, India, Mar. 2016, pp. 3561–3563, doi: 10.1109/ICEEOT.2016.7755367.
[24] J. C. S. Jacques, C. R. Jung, and S. R. Musse, "Background subtraction and shadow detection in grayscale video sequences," in *Proc. 18th Brazilian Symp. Comput. Graph. Image Process. (SIBGRAPI)*, Natal, Brazil, 2005, pp. 189–196, doi: 10.1109/SIBGRAPI.2005.15.
[25] R. Atmaja, M. Murti, J. Halomoan, and F. Y. Suratman, "An image processing method to convert RGB image into binary," *Indonesian J. Elect. Eng. Comput. Sci.*, vol. 3, no. 2, pp. 377–382, 2016. [Online]. Available: https://www.semanticscholar.org/paper/An-Image-Processing-Method-to-Convert-RGB-Image-Atmaja-Murti/4f6cd126dbbfe895dc4e835b314263d566143853, doi: 10.11591/ijeecs.v3.i2.pp377-382.
[26] L. Zhu, L. Liu, W. Jing, and J. Huang, "Contour extraction based on circular hough transform for forest canopy digital hemispherical photography," *Int. J. Performability Eng.*, vol. 14, no. 1, pp. 48–56, 2018, doi: 10.23940/ijpe.18.01.p6.4856.
[27] A. T. Peterson, J. Soberón, R. G. Pearson, R. P. Anderson, E. Martínez-Meyer, M. Nakamura, and M. B. Araújo *Ecological Niches and Geographic Distributions (MPB-49)*. Princeton, NJ, USA: Princeton Univ. Press, 2011. [Online]. Available: https://www.degruyter.com/view/product/451560

MUHAMMAD WALEED received the B.Sc. and M.Sc. degrees from the University of Engineering and Technology (UET) at Peshawar, Pakistan, in 2014 and 2017, respectively, where his master thesis was on the Quick Convergence of PSF estimation for Single Image Blind Deblurring. He is currently pursuing the Ph.D. degree with the Trust Data Analytics and Management Laboratory, Department of Information and Communication Engineering, Chosun University, South Korea.

His research interests include digital image processing, networking, big data, and machine learning particularly reinforcement learning for the optimization of the sensors power. He is also interested in future networks particularly cloud computing and mobile communication.

TAI-WON UM received the B.S. degree in electronic and electrical engineering from Hongik University, Seoul, South Korea, in 1999, and the M.S. and Ph.D. degrees from the Korea Advanced Institute of Science and Technology (KAIST), Daejeon, South Korea, in 2000 and 2006, respectively.

From 2006 to 2017, he was a Principal Researcher with the Electronics and Telecommunications Research Institute (ETRI), a leading government institute on information and communications technologies in South Korea. He is currently an Assistant Professor with Duksung Women's University, Seoul. He has been actively participating in standardization meetings including ITU-T SG 13 (future networks, including mobile, cloud computing, and NGN).

AFTAB KHAN received the B.E. degree in computer system engineering from the College of Electrical and Mechanical Engineering, National University of Sciences and Technology, Islamabad, Pakistan, in 2009. His Ph.D. thesis was on Single-Image Blind Deblurring and Restoration Techniques from The University of Manchester, U.K., in 2014.

From 2010 to 2013, he was a Graduate Teaching Assistant with The University of Manchester. He has been an Assistant Professor with the Department of Computer Systems Engineering, University of Engineering and Technology (UET) at Peshawar, Peshawar, Pakistan, since 2013. His image restoration expertise includes restoration of blurred images using blind deblurring techniques based on nonreference image quality measures. His image processing skills include OCT image denoising, medical image analysis, and image fusion. His research interests include digital image restoration, blind image deblurring, medical image processing, and digital image and video compression. He was a recipient of the Faculty Development Scholarship from UET at Peshawar, for his Ph.D. thesis.

ZUBAIR AHMAD received the bachelor's degree in mechatronics engineering from the National University of Science and Technology (NUST), Pakistan, and the master's and Ph.D. degrees from the University of Engineering and Technology (UET) at Peshawar, Peshawar, Pakistan, in 2012 and 2019 respectively.

He is currently working as a Lecturer with the Department of Mechatronics Engineering, UET at Peshawar. His research interests include robotics, artificial intelligence, computer vision, fault tolerant systems, and intelligent control systems.